

Study of glass-nanocomposite and glass–ceramic containing ferroelectric phase

E.K. Abdel-Khalek^{a,*}, E.A. Mohamed^b, Shaaban M. Salem^a, F.M. Ebrahim^a, I. Kashif^a

^a Department of Physics, Faculty of Science, Al Azhar University, Nasr City 11884, Cairo, Egypt

^b Department of Physics, Faculty of Science (Girl's Branch), Al Azhar University, Nasr City, Cairo, Egypt

ARTICLE INFO

Article history:

Received 24 May 2011

Received in revised form 4 December 2011

Accepted 21 December 2011

Keywords:

A. Glasses

C. Differential scanning calorimetry (DSC)

D. Optical properties

D. Ferroelectricity

ABSTRACT

Transparent glass nanocomposite in the pseudo binary system $(100 - x) \text{Li}_2\text{B}_4\text{O}_7 - x\text{BaTiO}_3$ with $x = 0$ and 60 (in mol%) were prepared. Amorphous and glassy characteristics of the as-prepared samples were established via X-ray powder diffraction (XRD) and differential scanning calorimetry (DSC) respectively. The precipitated BaTiO_3 nanocrystal phase embedded in the glass sample at $x = 60$ mol% was identified by transmission electron microscopic (TEM). The optical transmission bands at 598 and 660 nm were assigned to Ti^{3+} ions in tetragonal distorted octahedral sites. The precipitated $\text{Li}_2\text{B}_4\text{O}_7$, $\text{BaTi}(\text{BO}_3)_2$ and BaTiO_3 nanocrystallites phases with heat-treatment at 923 K for 6 h (HT923) in glass–ceramic were identified by XRD, TEM and infrared absorption spectroscopy. The as-prepared at $x = 60$ mol% and the HT923 samples exhibit broad dielectric anomalies in the vicinity of the ferroelectric-to-paraelectric transition temperature. The results demonstrate that the method presented may be an effective way to fabricate ferroelectric host and development of multifunctional ferroelectrics.

© 2011 Elsevier B.V. All rights reserved.

1. Introduction

Recently, transparent glass nanocomposites and glass–ceramics comprised of ferroelectric components in the nanometer range find a countless applications [1–4]. In addition to glass–ceramics are one type of interest hosts, as the glass matrix is favorable in its capability of fiber fabrication, in the meantime nanocrystals in glass–ceramics can provide active sites for transition metal (TM) ions [5]. Thus the luminescent properties of the optical materials are directly correlated with the valence state of the active ions such as Ni^{2+} [6]. From previous studies it is found that the transparent glass–ceramics are of interest as hosts for Ni^{2+} ions to realize ultra-broadband optical amplification [7–9]. Zhou et al. [10] showed that the nanocrystal-embedded hybrid materials are employed as hosts in order to take advantage of their convenience in local environment design for practical applications. Hao et al. [11] showed that the ferroelectric host (BaTiO_3) controls the luminescent properties of the optical materials through the change in the structural symmetry. Nowadays, the preparation of numerous ferroelectric materials by glass crystallization has been described in the literature [1,3]. Barium titanate (BaTiO_3) is a very important and interesting ferroelectric material for applications in electronic devices such as capacitors, electro-optic devices, radio communication filters [2,4]. BaTiO_3 has poor glass forming ability and high melting point thus in order to obtain a glassy material, it is usually required to add a glass former.

In the present study, we fabricate transparent glass nanocomposite and glass–ceramic in the pseudo binary system $(100 - x) \text{Li}_2\text{B}_4\text{O}_7 - x\text{BaTiO}_3$ with $x = 0$ and 60 (in mol%). The reason for choosing $\text{Li}_2\text{B}_4\text{O}_7$ is its relatively low melting point and its ability to form a glass readily by conventional melt quenching techniques [12]. In addition to $\text{Li}_2\text{B}_4\text{O}_7$ is a non-ferroelectric and piezoelectric material [13]. In order to obtain transparent glass nanocomposite, the nanocrystal phase embedded in the glass should be much smaller than the wavelength of the visible light (200 nm) [14]. The structural, optical and dielectric properties of the present samples have been studied.

2. Experimental

A transparent glasses with the molar composition $(1 - x) \text{Li}_2\text{B}_4\text{O}_7 + x\text{BaTiO}_3$ ($x = 0$ and 60 (in mol%)) were prepared by conventional melt quenching technique. The glass samples under investigation were prepared from reagent grade $\text{Li}_2\text{B}_4\text{O}_7$ (99.99%) and BaTiO_3 (99.99%). The batches were melted in a platinum crucible at 1100–1150 °C for 1 h. The melts were poured on to a copper plate and immediately pressed into plates. The differential scanning calorimetry (DSC) for glass samples were carried out on a SETARAM LabsysTM TG-DSC16 thermal analyser in the 303–1173 K temperature range. The as-prepared sample (at $x = 60$ mol%) was heat-treated in air, at 923 K (HT923) during 24 h. X-ray diffraction studies were performed at room temperature (RT) from a Siemens D5000 diffractometer using $\text{Cu K}\alpha$ radiation. Rietveld analysis of the diffraction data was performed using the FULLPROF program. High resolution transmission electron microscopy (TEM) studies

* Corresponding author.

E-mail address: Eid.khalaf0@yahoo.com (E.K. Abdel-Khalek).

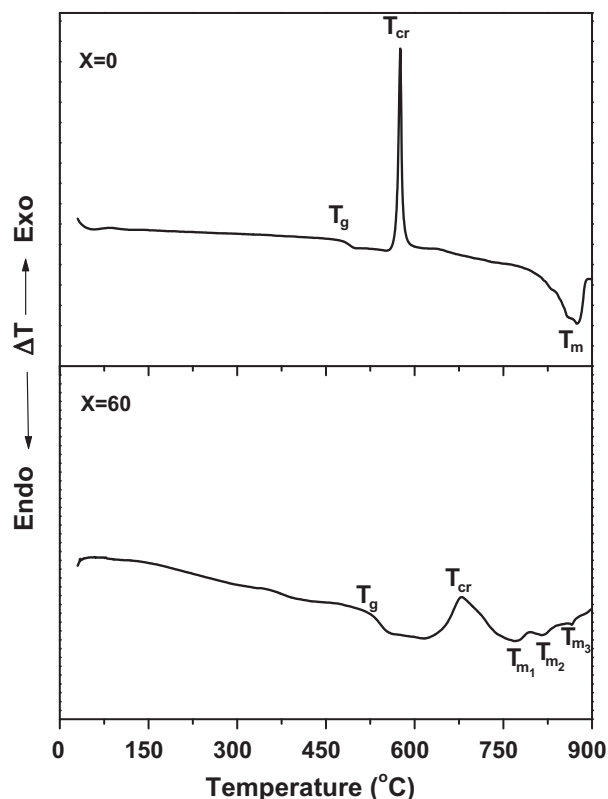


Fig. 1. Differential scanning calorimetry for the as-prepared samples.

were carried out on the as-prepared (at $x=60$ mol%) and HT923 samples. The IR absorption spectra of the glasses in the wavenumber range of $450\text{--}1600\text{ cm}^{-1}$ were recorded at room temperature on a Bruker (Vector 22), single beam spectrometer with a resolution of 2 cm^{-1} . The IR absorption spectra were recorded using KBr pellets. The optical transmission spectra of the as-prepared polished samples were recorded in the $200\text{--}750\text{ nm}$ wavelength range using a Hitachi 6405 spectrophotometer. Ac electrical conductivity and dielectric properties of the samples were measured as a function of composition, temperature and frequency. The ac data were collected using electronic RLC bridge type SR 720.

3. Results and discussion

3.1. DSC

Fig. 1 shows the DSC curves that were obtained for the glasses under investigation. The glass sample at $x=0$ mol% exhibits endothermic minima which represent the glass transition temperature T_g ($481\text{ }^\circ\text{C}$) and confirm the glassy nature of the sample. This sample exhibits also an exothermic peak T_{cr} ($575\text{ }^\circ\text{C}$) which due to the crystal growth followed by an endothermic effect due to the remodeling of the glass symbolized by T_m ($874\text{ }^\circ\text{C}$). The appearance of a single peak due to the glass transition temperature in DSC pattern of glass sample indicate the existence of high homogeneity in the glass sample [1]. The differential thermogram that was obtained for $x=60$ mol% shows a broad endothermic which represent the glass transition temperatures T_g at 533 and confirm the presence of the borate vitreous phase and titanate vitreous phase [15]. At still higher temperatures a broad exothermic peak T_{cr} ($678\text{ }^\circ\text{C}$) due to the crystal growth, followed by three endothermic effect at 756 , 820 and 866 which are related to the crystallization of different phases. The temperature difference between the T_g and T_{cr} ($DT=T_{cr}-T_g$), gives a measure for the thermal stability of the glass against

Table 1

Structural parameters for heat-treated (923 K/24 h) obtained from the structural refinement using X-ray powder diffraction data at room temperature.

Lattice constants	Atom	Site	Lattice coordinate		
			x	y	z
Tetragonal $\text{Li}_2\text{B}_4\text{O}_7$ ($I4_1cd$)					
$a=b=9.4608\text{ \AA}$	Li	16b	0.21102	0.26737	0.85901
$c=10.2768\text{ \AA}$	B1	16b	0.08663	0.16475	0.22896
	B2	16b	0.18005	-0.06861	0.11834
	O1	16b	0.14193	0.28504	0.25570
	O2	16b	0.17140	0.01104	0.14720
	O3	8a	-0.06105	0.15917	0.18006
Rhombohedral $\text{BaTi}(\text{BO}_3)_2$ ($R\bar{3}$)					
$a=b=5.0005\text{ \AA}$	Ba	3a	0.00000	0.00000	0.00000
$c=16.3744\text{ \AA}$	Ti	3b	0.00000	0.00000	0.50000
	B	6c	0.00000	0.00000	-0.22520
	O	18f	0.31320	0.12710	-0.23650
Tetragonal BaTiO_3 ($P4mm$)					
$a=b=4.3178\text{ \AA}$	Ba	1a	0.00000	0.00000	0.00000
$c=4.1061\text{ \AA}$	Ti	1b	0.50000	0.50000	0.48530
	O	1b	0.50000	0.50000	0.00210
	O	2c	0.50000	0.00000	0.50910
Phasefraction (%)					
Tetragonal ($I4_1cd$)			Rhombohedral $R\bar{3}$	Tetragonal ($P4mm$)	
81.14			11.76	7.10	

crystallization [16,17]. The DT value increases with introducing BaTiO_3 . It can also be seen that the width of exothermic peak increases with introducing BaTiO_3 . This widening may be attributed to the slowing down of crystallization process [18].

3.2. X-ray diffraction and TEM studies

The XRD patterns that were obtained for the as-prepared at $x=60$ mol% as well as HT923 samples are depicted in Fig. 2. As shown in Fig. 2(a) the XRD pattern exhibits a broad hump without any distinct peak in the as-prepared at $x=60$ mol% indicates the amorphous nature. Rietveld refinement of the data Fig. 2(b) reveals that the sample crystallizes in an tetragonal ($I4_1cd$) $\text{Li}_2\text{B}_4\text{O}_7$, rhombohedral ($R\bar{3}$) $\text{BaTi}(\text{BO}_3)_2$ and tetragonal ($p4mm$) BaTiO_3 consistent with the previously reported results [3,19,20]. But there is a noticeable shift in the peak positions than those of the pure powder sample of $\text{Li}_2\text{B}_4\text{O}_7$, $\text{BaTi}(\text{BO}_3)_2$ and BaTiO_3 . This can be attributed to the existence of uneven distribution of strain which arising out of the anisotropic growth of $\text{Li}_2\text{B}_4\text{O}_7$, $\text{BaTi}(\text{BO}_3)_2$ and BaTiO_3 crystals in glass matrix [3]. The quantitative phase analysis of powders and refined values of the lattice and positional parameters at room temperature are summarized in Table 1. The broad nature of the diffraction peaks in Fig. 2(b) indicates that the presence of very fine crystallites of $\text{Li}_2\text{B}_4\text{O}_7$, $\text{BaTi}(\text{BO}_3)_2$ and BaTiO_3 [10]. It is also noted that there are $\text{Li}_2\text{B}_4\text{O}_7$, $\text{BaTi}(\text{BO}_3)_2$ and BaTiO_3 crystals in glass matrix is not perfectly stoichiometric, but contains a certain amount of oxygen vacancies where vacancies are formed after the removal of oxygen atoms that bridge the adjacent tetrahedra, resulting in the formation of distorted octahedral environments [10].

The transmission electron micrographs recorded for the as-prepared at $x=60$ mol% as well as HT923 samples are shown in Fig. 3. The micrograph recorded for the as-prepared glass (Fig. 3(a)) shows its overall amorphous nature with the presence of small BaTiO_3 nanoclusters which precipitated during glass formation. Hence the as-prepared sample at $x=60$ mol% is a glass-nanocomposite. These small BaTiO_3 nanoclusters are not clearly detected from the XRD patterns. These results are due to their low concentrations (low for X-ray detection) embedded in the glass matrix and small size also [3,21]. These nanoclusters are not clustered in one portion of the glass but scattered all over the

Download English Version:

<https://daneshyari.com/en/article/1524178>

Download Persian Version:

<https://daneshyari.com/article/1524178>

[Daneshyari.com](https://daneshyari.com)